Research activities on INCE/J RTV (Road Traffic Vibration)-Model Part: 1 Prediction of road traffic vibration for elevated roads

Masayuki SHIMURA[1]; Noboru KAMIAKITO[1]; Saiji FUKADA[2]; Yasuyuki SANO[3];
Yasunao MATSUMOTO[4]; Toshikazu OSAFUNE[5]; Hiroshi IWABUKI[5];
Akito YABE[6]; Hirokazu HAMA[7]

[1]Civil Engineering and Eco-Technology Consultants, Japan; [2]Kanazawa University, Japan;
[3] Aichi Institute of Technology, Japan; [4]Saitama University, Japan;
[5]Nippon Expressway Research Institute, Japan;
[6]KKE Inc., Japan; [7]Fujiengineering Co., Japan

ABSTRACT

There have been an increasing number of complaints from residents living along sides of highways about noise and vibration. Especially, ground vibration and low-frequency sound generated from bridges which are related to various factors such as bridge structures, ground conditions and traffic load. Therefore, the problems originated from this complex phenomenon are hardly solved. Concerning about vibration problem, this may be a problem only happened in Japan because of uniquely light-weight house lined close to the road.

The committee of Japan Noise Control Engineering Society has published a version of road traffic vibration prediction formula named "INCE/J RTV-Model 2003". At present, this version is highly applicable for flat roads, but not for cutting-structure roads, banking-structure roads, and elevated roads. The objective of this report was to introduce research results of the working group (WG) related to elevated roads. In addition, results of performing the numerical simulation and extensive experiment on operated highways were shown.

Keywords: Bridge, Transmission, Vibration   I-INCE Classification of Subjects Number(s): 40

1. INTRODUCTION

When a large vehicle runs on an elevated road, the vehicle-induced vibration is excited by steps and uneven road surface. Furthermore, it raises more vibration and coupled oscillation of the elevated road. The ground vibration to the surrounding environment of the road and the vibration of the elevated road that combined/resonated with the vibration of vehicles are propagated at low-frequency sound and noise. If the vibration/noise receiving point is in a house (floor, joinery, human body, etc.) and near the vibration source of elevated road, and a number of complaints about low-frequency of noise and vibration have been increasing, generally, it is called environmental vibration of elevated roads. Factors that affect environmental vibration are: behavior of road surface, various elements of super- and lower-structures of the elevated road, and characteristics related to exciting force of the vehicle. In order to establish the vibration propagation mechanism for elevated road, traffic vibration WG in INCE/J have conducted a large-scale experiment by using the actual highway, and attempted a numerical simulation.

1 shimura@kensetsukankyo.co.jp
2 saiji@t.kanazawa-u.ac.jp
3 sano-y@aitech.ac.jp
4 ymatsu@mail.saitama-u.ac.jp
5 t.osafune.aa@ri-nexco.co.jp
6 akito-yabe@kke.co.jp
7 hirokazu_hama@fujiengi.co.jp

2. FIELD EXPERIMENTS

2.1 Static Loading Experiment

A large vehicle (net weight about 25tons) which was used for the static loading experiment is shown as follows. The experiments were conducted on continuous 10-span bridge with two-steel main girders.

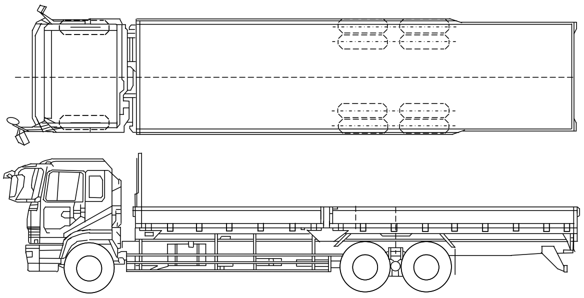

Figure 1 – Model of a large vehicle

Table 1 – Specifications of the vehicle

	Items	Unit	Values
Length	Wheel pitch A	m	5.72
	Wheel pitch B	m	6.38
	Rear shaft pitch	m	1.32
	Wheel shaft length	m	1.94
Weight	Front wheel weight	kN	66.54
	Rear wheel weight (front shaft)	kN	88.89
	Rear wheel weight (rear shaft)	kN	90.45
	Total weight	kN	245.88

One of the measurement results for deformation of main girder is shown in Figure 2, where the horizontal axis represents the position of the front tire and the vertical axis denotes the vertical displacement of the measurement points at the span-center of the each girder. Based on these results we estimated the elasticity for the superstructure of the bridge. The arrows in the figure designated the position of the piers, and there was an expansion joint at AP30.

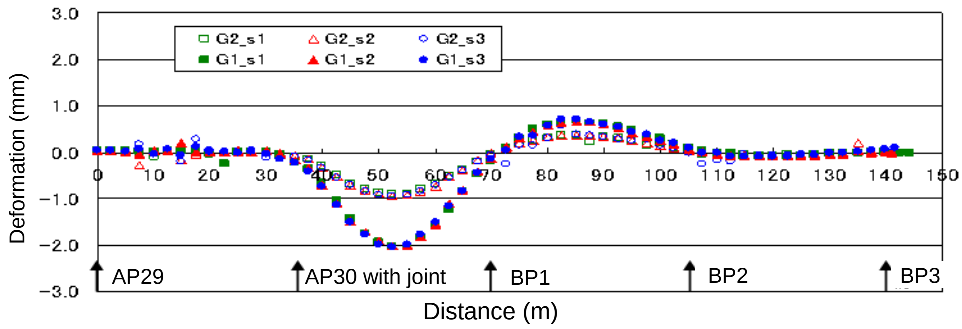

Figure 2 – Displacement (Z) of the span-center

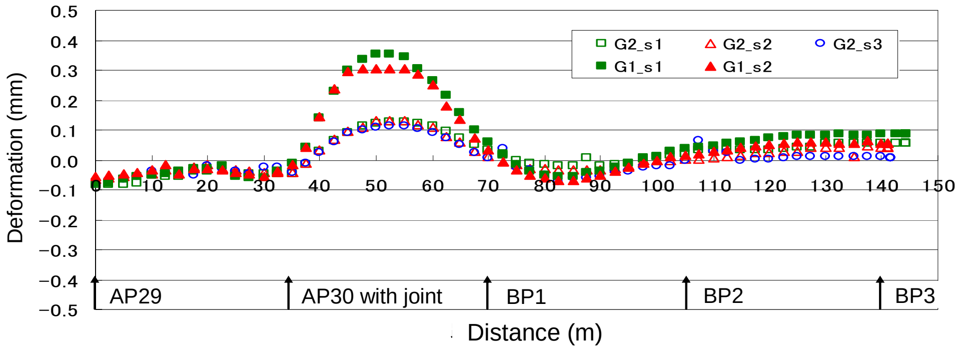

Figure 3 – Displacement (Y) of rubber bearing with expansion joint

2.2 Static Loading Experimental Results

In order to grasp static behavior we carried out a quasi-static loading examination. As a result, the bends of the main girders were 1mm and 2mm for the sides of G2 girder and G1 girder, respectively. In addition, the bending span between the AP30 - BP1 caused a bend when a vehicle moved over AP30 – BP3 because of the continuous girders. Displacement at the rubber bearing position was larger in bridge axis direction. And the displacement at the rubber bearing position with expansion joint was also largest. Displacement of the perpendicular direction was perhaps depending on the local shear deformation or relative displacement of rocking mode.

2.3 Impact Loading Experiment

Impact loading points and the measurement points for acceleration are shown in figure 4 and 5 respectively. The impact load source was the same as the static loading experiment.

Figure 6 shows the spectrum due to the acceleration wave-pattern of span points of 1/2 and 1/4 above G1 girder when the test vehicle was impact loading at 1/4 point of span length AP30-BP1. From this, dominant frequency was observed in the vicinities of the span 1/2 point, about 3Hz and the span 1/4 point, about 10-15Hz.

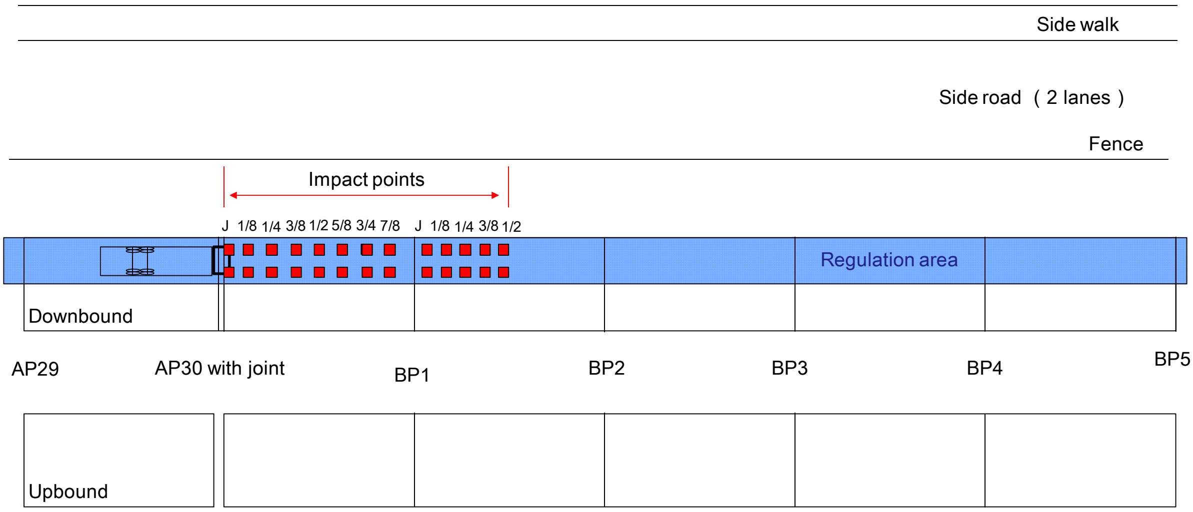

Figure 4 – Impact loading points

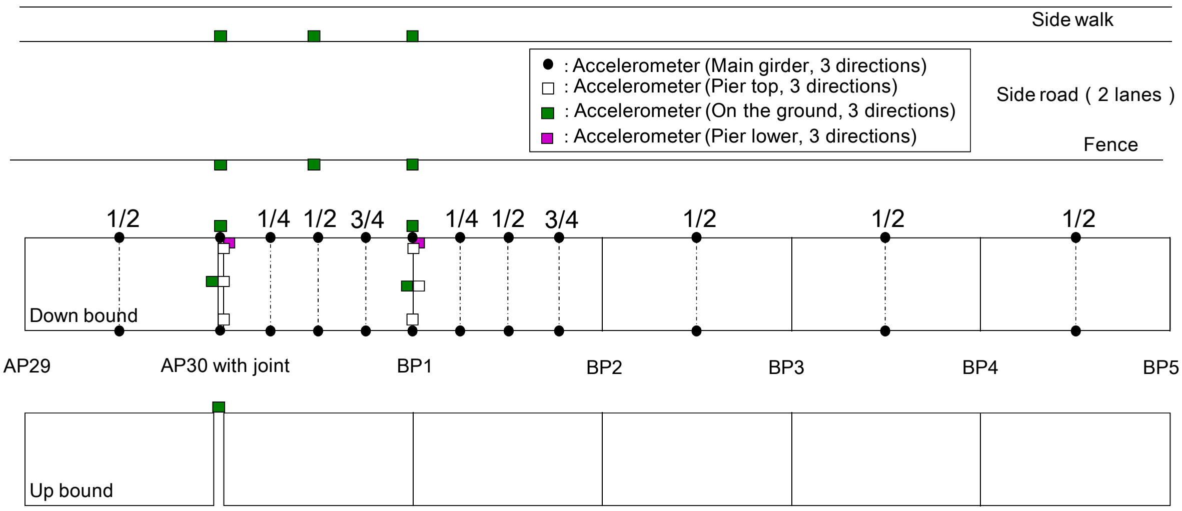

Figure 5 – Measurement points

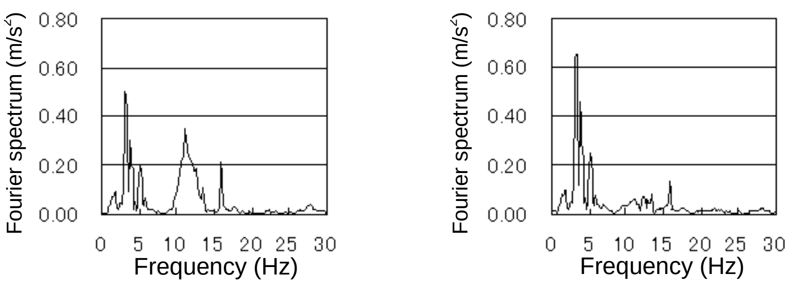

(a) 1/4 point on G1girder (b) span center on G1 girder

Figure 6 – Fourier spectrum of measured results at main girder

Because the damping constant changes according to the vibration mode, we had decided to check wave pattern analysis and filtering process applying the scheme of reference 3. Here, as those obtained results, vibration mode of about 3Hz (primary mode shape) and vibration mode of about 10Hz (secondary mode shape) are shown in Figure 7 and Figure 8, respectively. In addition, the analysis mode shape by the natural frequency analysis as the reference was added. From this, it can be seen that the vibration modes of the experiment and analysis were almost the same. Furthermore, in this target elevated road, because of 10 continuous spans, besides the above-mentioned modes, a lot of vibration modes in 3-4Hz, 10-11Hz existed as well.

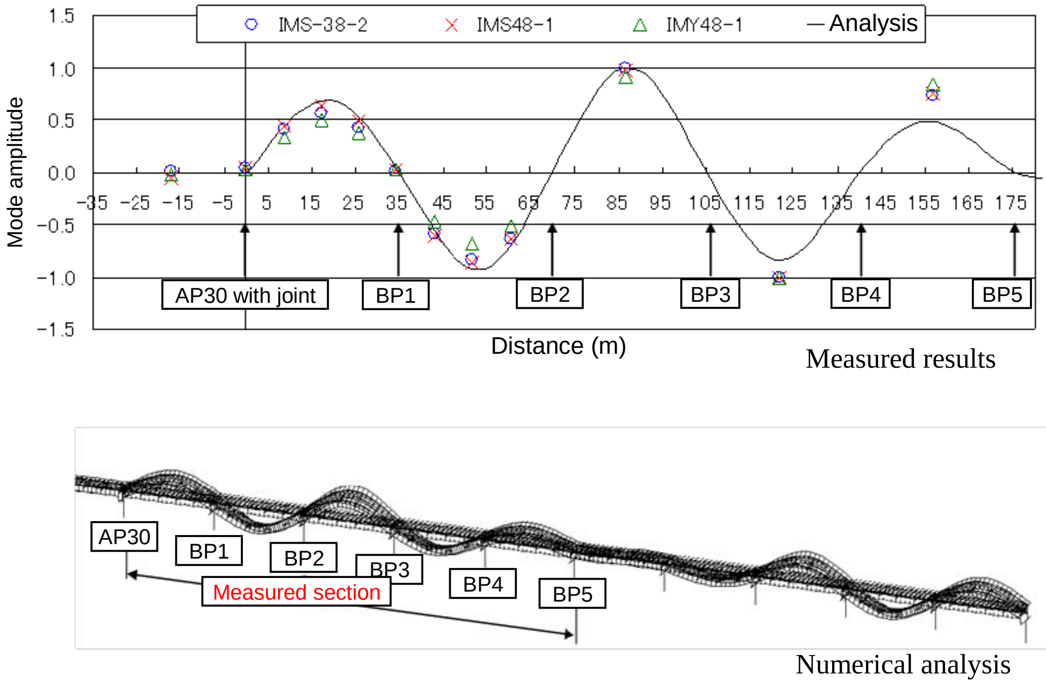

Figure 7 – Mode shape analysis by measurement results (3Hz)

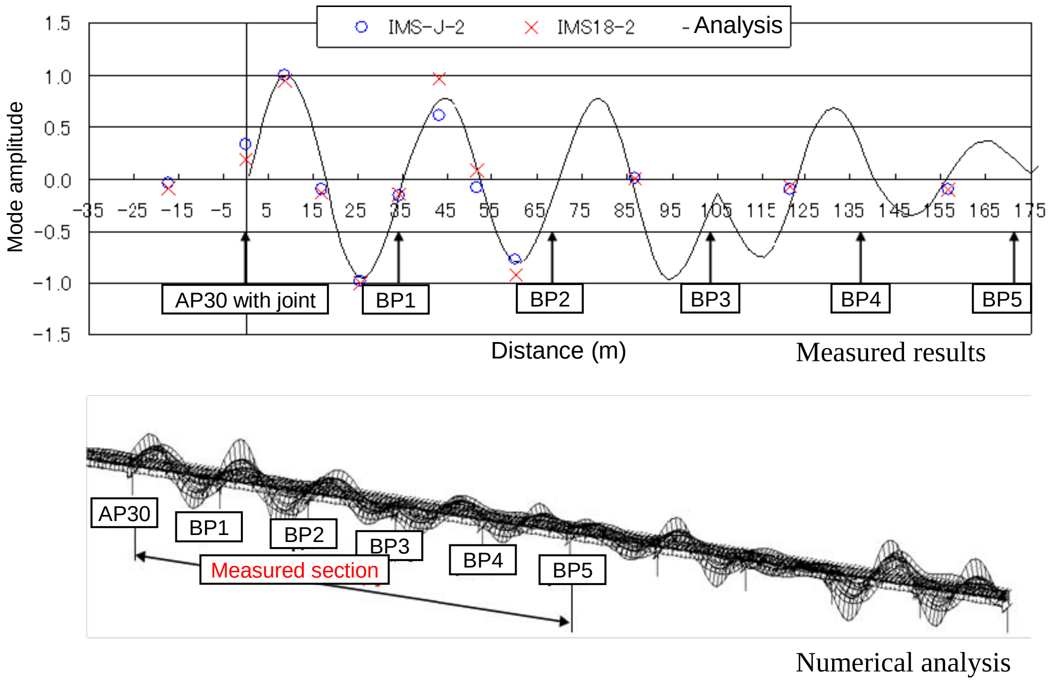

Figure 8 – Mode shape analysis by measurement results (10Hz)

2.4 Impact Loading Experimental Results

To understand the dominant frequency of the superstructure in the target bridge, vibration modes were gasped. In addition, to understand the properties of vibration propagation to the neighboring ground from superstructure and substructure, we conducted impact loading experiments using a test vehicle. Great excellence was observed at 1/4 point of span, about 10-15Hz and at 1/2 point of span, about 3Hz. After analysis of the mode damping, the results were: damping rates of 1-2% and 2-3% for about 3Hz and about 10Hz, respectively.

2.5 Propagation Properties by Impact Loading

At the pier top (AP30 with joint), in the vertical direction and direction perpendicular to the bridge axis, as mentioned above, bending vibration of the primary mode about 3Hz and the secondary mode about 10Hz was predominant. In particular, at excitation span points of 1/8 and 3/4, because of vibrating the central and abdominal vicinity of the secondary mode, predominant of about 10Hz was higher. Further, the excitation at span point 1/2, because of vibrating the center of the primary mode shape and bending, vibration about 3Hz was larger than about 10Hz. In addition, in the target bridge, despite of excitation to the vertical direction because of crossing slopes, the same level of response to vertical direction and direction perpendicular to bridge axis had been observed. Further, as described in the quasi-static loading test, because the displacement also occurs in the bridge axis due to deformation and bending, in particular, at the primary bending vibration, bridge axis vibration excelled greatly. At the lower end of pier (AP30 with joint), compared to the frequency characteristics of the predominant frequency of pier top end as it propagated, Fourier amplitude was 30-40% smaller. Similarly to the pier top end, excitation at span points of 1/8 and 3/4, on vertical direction, vibration about 10Hz became larger more than excitations at other points. On the ground, 5 m away from the pier (AP30 with joint), compared to the lower end of the pier, at any excitation time, amplitude of 3Hz vibration was reduced, meanwhile it was increased for 10Hz vibration and this case frequently happened. In the vertical direction, 10m above the ground, 10Hz vibration was amplified, and different frequencies of about 10-15Hz were activated. Also, at each time of excitation, at 10m above the ground point, within 3 directions, vibration in the vertical direction had been observed highest. Further, in the vertical direction, 10m above the ground, with excitation at 1/2 point, new 5-10Hz frequencies appeared but no vibration was observed on the bridge.

At the pier top end (BP1 no joint), the same as pier lower end (AP30), vibration modes of the primary bending about 3Hz and the second bending about 10Hz were distinguished. At pier lower end (AP30), excitation at span points of 1/8 and 3/4, the 10Hz vibrations in the vertical direction and the direction perpendicular to the bridge axis were distinguished. On the other hand, the 3Hz vibration was predominant in the bridge axis direction in this pier. In particular, the excitation at point 1/2 span, for vibrating the belly of the primary mode shape bend, this tendency was remarkable. Also, it was considered that the vibration mode of the primary shape bending was excited because many frequencies were dominant about 3Hz. At the lower end of pier (BP1 no joint), as the same way as (AP30) pier lower end, the frequency characteristic of the predominant frequency in pier top end is propagated as it was, Fourier amplitude was 30-40% smaller. Similarly to the pier top end, the vibration of bridge axis direction about 3Hz was predominant. From the pier end point 5m on the ground, compared to lower end of the pier, for the any case of excitation, dominance was reduced at about 3Hz, whereas 10Hz frequency band was dominant. In the vertical direction, 10m from the pier, dominance was larger than that of the other two directions, and was amplified more than at 5m point. In addition, as observed at the end of piers, new dominance of excitations at span points 1/4 and 1/2 was observed, and dominated by amplifying rather than at 5m point.

2.6 Running Load Experiment

In figure 9, the measurement points are shown for the case of running load experiment by a test vehicle to understand the mechanism of vibration propagation from superstructure to ground via substructure. Total channel numbers for simultaneous measurement were 122ch at superstructure, substructure and ground.

2.6.1 Experiment with Test Running Vehicle

To understand the vibration propagation characteristics, the experiment was conducted using test running vehicle, based on differences in the driving pattern of the vehicle. If looking at waveform by time, vibration shocking occurred in the joint at the time of passing over the step. Shocking waveform variation was observed, especially at high frequency. For band 3Hz-4Hz which was considered the primary natural frequency of superstructure, shocking change was rarely observed. Looking at the unit pattern, even at any unit pattern, in the high frequency range of 63Hz, there was a change in shocking level. Unit pattern was measured according to the front wheel position, but when the rear wheels pass through joints, the shocking vibrations become high. Vibration acceleration level became highest at the time when the rear wheels of the test car pass the joint, not the front wheels.

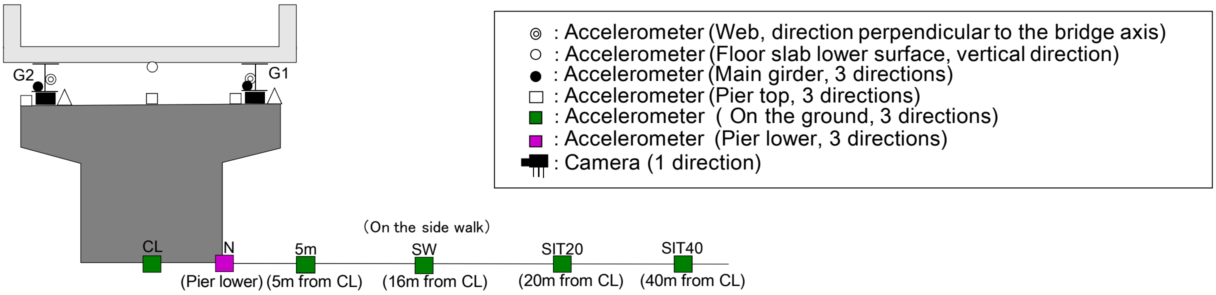

Figure 9 – Description of measuring points

2.6.2 Running Load Experimental Results

For band 3Hz-4Hz of the natural frequency domain of a superstructure, while there was a vehicle on this superstructure, the tendency indicating a steady value was recognized. The primary natural vibration excited by the test vehicle in the test area（AP-30～BP-5）on superstructure separated by joints was almost steady, because this is a phenomenon in which entire bridge is resonant. When the vibration acceleration level is analyzed by the maximum value L_{VAMax}, at the survey point near the piers in Y direction which is horizontal direction of the bridge axis, measured acceleration was big. For the measurement point at 20m away from running cars, the influence of vertical vibration was large.

According to results of FFT analysis, dominant vibration of 3Hz was observed at any measurement point. This is believed to be the primary natural frequency component of the superstructure.

Looking at the maximum value of ground vibration L_{VAmax}, we could understand the reason for vibration complaints. Vibration can be felt when it exceeds 55dB ~ 60dB, but the vibration measurement result was 10dB smaller than its exact value. By comparing the vertical and horizontal direction, towards the vertical direction (Z-direction), measured vibration was almost the same as felt vibration.

We have attempted to estimate the mechanism of vibration propagation for maximum levels. As a result, the vibration of 3.15Hz band became big in the vertical direction (Z-direction) at measurement point of 2/4 girder. Then, vibration at measurement points of 1/4, 3/4 was increased. Because of a fulcrum on top of the pier, measurement points AP-30 and BP-1 had smaller values of vibration. We considered the vibration of 3.15 Hz was the primary bending vibration of the superstructure. This vibration propagated through rubber bearing position to pier top and grew big in horizontal direction of bridge axis (Y-direction). For the domination of 16Hz vibration, it is thought that the domination in vicinity of span center of the girder was caused by a vibration mode in direction perpendicular to the bridge axis (X-direction). The vibration on the pier top increased toward horizontal direction perpendicular to the bridge axis (Y-direction) and propagated towards pier and the ground.

An effort has been made to estimate the vibration generating mechanism based on unit pattern. As a result, vibration in the vertical direction (Z-direction) was larger than other directions (X-direction, Y-direction), and a difference of more than 10dB occurred after the test vehicle has just passed. When a big vehicle run over the expansion joint point of 0m, no big vibration occurred, and on the ground, from 15m far away from central point of AP-30 and BP-1, big vibrations started to occur. From the next pier of AP-30, when the test vehicle runs over BP-1 to BP-30, there was constant vibration. In the primary bending of the superstructure, when the test vehicle was on the superstructure, the trend that vibration actively continued was observed. We analyzed the unit pattern of octave band 16Hz （12.5Hz～20Hz）. As the results of comparing with the vertical direction (Z-direction) and the bridge axis direction (Y-direction), the vibration that perpendicular to bridge axis (X-direction) was more than 15dB larger. A big test vehicle passed through the joint of 0m, acceleration level rose due to passing over the step. Moreover, level rose in the span center, the vehicle moves away, the trend of vibration reducing was observed. Joint step also influenced to some extent for the bandwidth of 16Hz, it was believed that span portion passing could be the main element affecting generated vibration.

2.7 Vibration Transmission

2.7.1 Vibration Propagation Characteristics

We analyzed the vibration propagation of each octave band. When vibration propagates from superstructure to pier top end, trend of attenuation for each frequency band was observed. On ground surface near the lower end of piers 5m from foot of pier foundation, vibration affected surrounding houses, and though there were slight changes in the band of 14~16Hz, generally, constant values were obtained.

For the distance more than 5m, even though a little bit change was observed, and there was the tendency of attenuation by distance. For the low frequency band about 4Hz, geometric attenuation was 3dB by double distance. For the higher frequencies of 32Hz band, geometric attenuation was 6dB by double distance. The propagation characteristics of the vibration acceleration maximum value L_{VAMax} were investigated. For the vertical direction, with frequency less than 10Hz, vibration was attenuated about 5dB and it became reduced of 10dB in the frequency range higher than that. For the bridge axis direction (Y), a band of 8Hz and 16Hz was amplified. Vibration with frequency band of 3Hz - 12Hz on elevated road was a problem in the residential area, and high frequency amplification was observed.

2.7.2 Comparison of the Running Case

The vibration acceleration far from the pier with joint 16m on the ground became large for any running case (driving lane, passing lane, running speed 80 or 90km/h), at any frequency band of about 4Hz, 16Hz, and 50Hz. The vibration acceleration far from the pier without joint 16m on the ground became large for any running case (driving lane, passing lane, running speed 80 or 90km/h), at frequency band of about 16Hz and 50Hz, however vibration of 4Hz band was not dominant.

3. NUMERICAL SIMULATION

3.1 Measuring of the Traveled Surface Characteristics

We could evaluate the measurement results of traveled surface roughness by applying International Roughness Index, consequently the repair critical value of NEXCO was 3.5mm/m as IRI-200, the measured results was less than the critical values as shown in Figure 2. The traveled surface characteristics of the road were in good condition.

Figure 10 – Measuring car for roughness of road surface

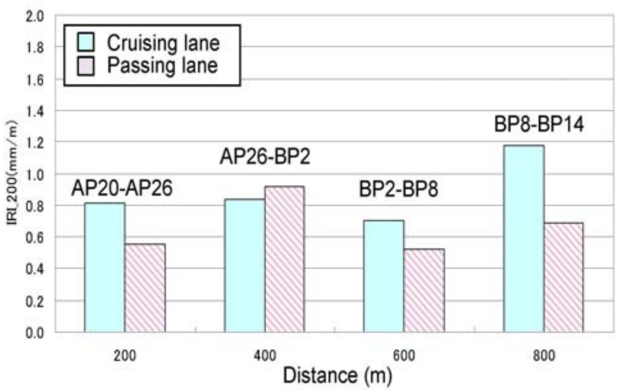

Figure 11 – Measured results

3.2 Modeling of the test running vehicle

The modeling of test running vehicle is shown in Figure 12, where the model has 12 nodes in 3 dimensions, and the values of specifications were used as the same values in Table 1.

It has been recognized that natural frequencies were concentrated into 11Hz-12Hz by the eigenvalue analysis. These frequencies were dominant for interaction force between the vehicle and surface roughness.

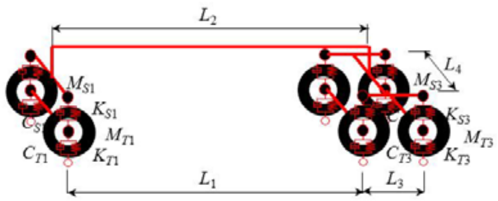

Figure 12 – Modeling of the test running vehicle

3.3 Finite Element Model for the Elevated Road

This bridge was installed of 2 main girders, and made of composite slab deck. The upper deck had 4% gradient in cross section as shown in Figure 13. Considering these characteristics, finite element model was constructed. Second order plate bending element was adopted for web plate of main girder, upper deck, cross beam, railing and sound barrier. For the flange of main girder, cross beam on middle position and support components of sound barrier, beam elements were applied. Total model length of the elevated road was 352.9m (10 spans). The foundations which have five piles were modeled as rocking freedom in bridge axis (Y) and perpendicular axis (X).

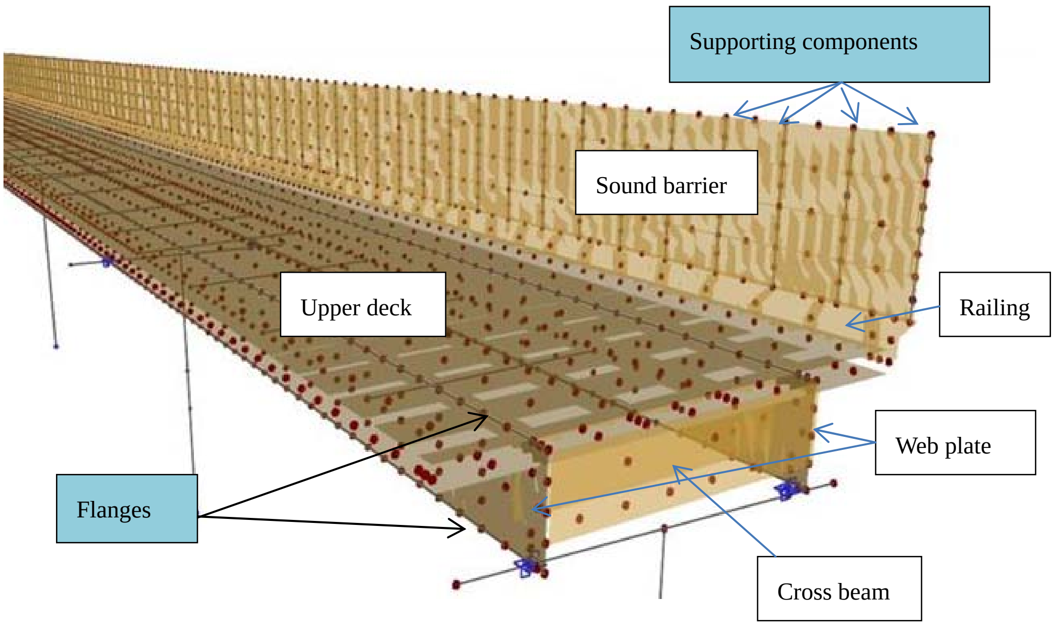

Figure 13 – Finite element model

3.4 Numerical Results

Numerical results are shown in Figure 14 comparing with measured results. Upper figures are time historical acceleration response of measurement and calculation points and lower figures denote the Fourier spectrum for each result. The results of span center and 5m point on the ground surface were considered as examples. Numerical simulation using finite element method was in good accordance with measured results.

Visualization of these results will be shown as animations in the conference.

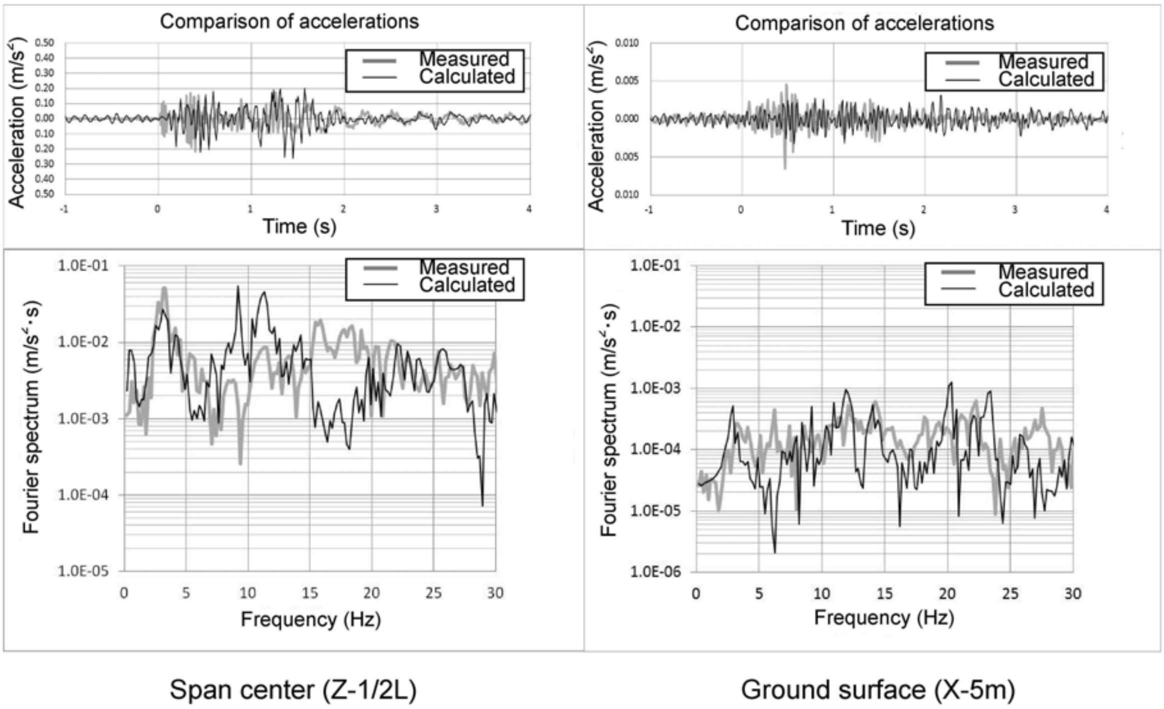

Figure 14 – Comparison between calculation and measurement results

4. CONCLUSIONS

Through these experiments and large scale numerical simulations for the elevated road, our conclusions are as follows.

1) Load-displacement relation was obtained by the static loading experiment for a new existing elevated road in practical use, and these results were corresponding to the primary bending mode of each span.

2) It can be seen by the running load experiment that primary bending mode of the span always occurs such as standing wave while the large vehicle is running on the elevated road with continuous girders. At the expansion joint, the wave motion is discontinuous. It is possible to abate by TMD (tuned mass damper) for instance, for primary mode to some extent, because the primary mode of the bridge span continues to vibrate in time domain.

3) By applying the impact load experiment moving the excitation points, higher mode shape 10Hz-12Hz and its damping coefficient were obtained.

4) Higher vibration modes of 10Hz-12Hz are dominant when the vehicles pass on the expansion joint. This phenomenon is an interaction problem between the suspension/tire of vehicle and expansion joint step. If the main girder is continuous, the shock vibration is smaller. And these frequency domains with resonance of vibration are sometimes to blame for wobbling the windows, light partitions or furniture in residential dwelling nearby.

5) Quantitative influence of expansion joint for vibration generation was investigated that there was difference in peak level for each frequency band.

6) Large-scale numerical simulation using finite element method was successful for the vibration propagation from superstructure to ground. However more improvements for the modeling and adaptability are necessary.

5. NEAR FUTURE WORKS OF THE INCE/J WG

Our final goal is to establish the prediction method which is applicable to road traffic vibration abatement and environmental assessment. Further research related to this study should be conducted, for example: dynamic interaction between foundation of the pier and soil, the modeling of excitation force by running vehicle, numerical simulation modeling and so on.

For the foundation-soil interaction problem, we have already gathered the measured data for many types of elevated road’s piers in Japan, and the analysis is on progress. In near future we will present the new modeling on the interaction subjects.

For the prediction method of environmental vibration from road traffic, we are considering the more concise method without large scale computations.

REFERENCES

1. Hidenobu Uchida, Akinori Yokota, Yasuyuki Sano and Haruoki Naruse: Prediction model "INCE/J RTV-Model 2003" for ground vibration caused by road traffic, Part 1: outline of the prediction model, Inter-noise, 3-6 Dec. 2006
2. Yasuyuki Sano, Tatsuo Miyake, Hidenobu Uchida and Haruoki Naruse: Prediction model "INCE/J RTV-Model 2003" for ground vibration caused by road traffic, Part 2: Procedure for calculation, Inter-noise, 3-6 Dec. 2006
3. Juang, J. N. and Pappa, R. S.: An Eigensystem Realization Algorithm for Modal Parameter Identification and Model Reduction, Journal of Guidance, Vol.8, No.5, pp.620-627, Sept.-Oct., 1985.